NANO LETTERS

Letter

pubs.acs.org/NanoLett

Tuning Rectification in Single-Molecular Diodes

Arunabh Batra,[†] Pierre Darancet,[†,§] Qishui Chen,[‡] Jeffrey S. Meisner,[‡] Jonathan R. Widawsky,[†] Jeffrey B. Neaton,[*,§] Colin Nuckolls,[*,‡] and Latha Venkataraman[*,†]

[†]Department of Applied Physics and Applied Mathematics, Columbia University, New York, New York 10027, United States

[‡]Department of Chemistry, Columbia University, New York, New York 10027, United States

[§]Molecular Foundry, Lawrence Berkeley National Laboratory, Berkeley, California 94720, United States

Supporting Information

ABSTRACT: We demonstrate a new method of achieving rectification in single molecule devices using the high-bias properties of gold−carbon bonds. Our design for molecular rectifiers uses a symmetric, conjugated molecular backbone with a single methylsulfide group linking one end to a gold electrode and a covalent gold−carbon bond at the other end. The gold−carbon bond results in a hybrid gold-molecule "gateway" state pinned close to the Fermi level of one electrode. Through nonequilibrium transport calculations, we show that the energy of this state shifts drastically with applied bias, resulting in rectification at surprisingly low voltages. We use this concept to design and synthesize a family of diodes and demonstrate through single-molecule current−voltage measurements that the rectification ratio can be predictably and efficiently tuned. This result constitutes the first experimental demonstration of a rationally tunable system of single-molecule rectifiers. More generally, the results demonstrate that the high-bias properties of "gateway" states can be used to provide additional functionality to molecular electronic systems.

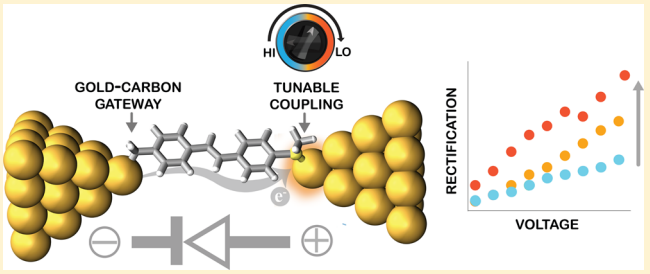

KEYWORDS: *Molecular diode, gold−carbon covalent bonds, single-molecule rectifier, density functional theory*

The experimental demonstration of a single-molecule diode is a first step toward the goal of creating functional molecular electronic devices and has generated substantial interest since Aviram and Ratner first proposed their elegant design for a molecular rectifier.[1] However, experimental realizations of this[2] and other diode schemes[3,4] at the single-molecule level have been limited by poor predictability of performance and extreme sensitivity to molecular design.[5,6] Over the past few decades, single-molecule electronics has made significant progress in relating the chemical structure of molecules to their electronic properties.[7−9] The ongoing challenge is to create higher electrical functionality through molecular design, thus going beyond the use of molecules as merely resistive elements. The earliest proposal for such a device is the Aviram−Ratner diode,[1] which involves a donor−σ−acceptor molecule connected symmetrically to two metal termini. The conceptual simplicity of this design belies some fundamental limitations.[3,6,10] First, the characteristics of such donor−acceptor diodes are very sensitive to the energy level alignment of the molecular orbitals with each other, and with the connecting electrodes, making experimentally predictable designs difficult.[11,12] Second, rectification in such diodes requires a σ bridge, which effectively adds a large tunnel barrier to the backbone and results in very large junction resistance. As a result, the few experiments that have demonstrated functional single-molecule diodes all have resistances greater than 10 MΩ.[2,4,13] To date, the only experimentally realized alternatives to donor−acceptor type diodes have been "many-molecule" devices where one linker group is eliminated[14,15] or weakened,[16,17] creating an asymmetrically contacted junction.[18−20] These junctions do not have well-defined molecular geometries and show low conductances, making measurements at the single-molecule scale difficult.[3,20] In addition, experimental realizations of molecular rectifiers have so far operated at relatively high biases[2,4] of >1 V. In these voltage regimes, the room-temperature stability of single-molecule junctions becomes a limiting factor. To overcome these shortcomings, we have explored a new method of achieving rectification using the electronic properties of molecular junctions with highly conducting covalent gold−carbon bonds. We demonstrate that this new family of molecular diodes exhibits high electrical conductance and high rectification at low bias and can be efficiently and predictably tuned.

Our proposed rectifier design (molecule **1**, Figure 1a) consists of a stilbene molecular backbone with a single methylsulfide linker[21] at the 4 position (red circle) and a covalent gold−carbon bond at the 4′ position (green circle), formed in situ through the benzylic trimethyltin functionality[22] (see Supporting Information (SI)). We measure the con-

Received: October 3, 2013
Revised: November 12, 2013

   dx.doi.org/10.1021/nl403698m | *Nano Lett.* XXXX, XXX, XXX−XXX

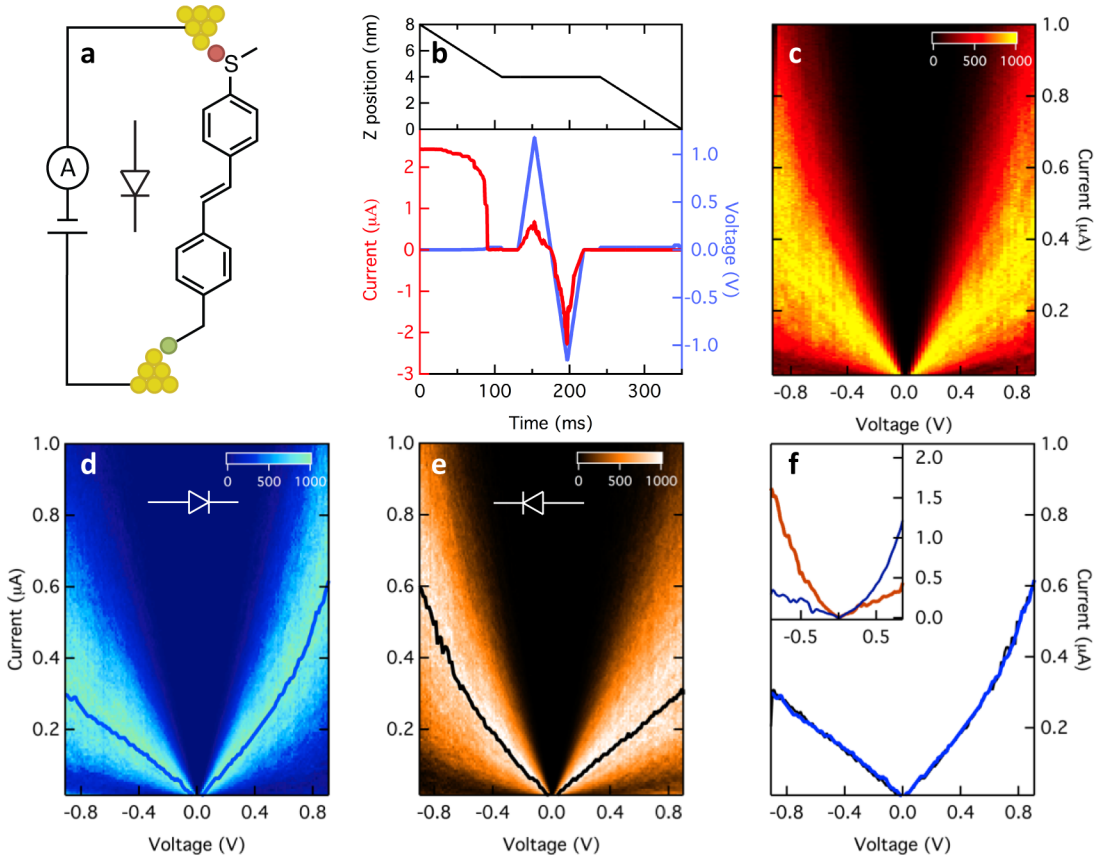

Figure 1. (a) Schematic for molecular circuit formed by molecule **1** between two gold electrodes, with the carbon−gold bond represented by a green circle and methylsulfide-gold bond represented by a red circle. A diode circuit element is shown to highlight the directional asymmetry of this circuit. (b) Representative current, voltage, and displacement (z-position) traces for a single break junction measurement. The $I-V$ ramp is applied when z is held constant. (c) Two-dimensional histogram made up of thousands of traces similar to those shown in b; no asymmetry is seen because the orientation of molecule in junction is not controlled. (d) Forward bias and (e) reverse bias two-dimensional histograms recovered from c, using trace sorting. Blue (forward) and black (reverse) line fits define average $I-V$ curves from the histogram distributions. (f) Average $I-V$ curves for d and e, overlaid with the reverse bias (black) curve mirrored across the vertical axis. Average rectification ratio is 1.7 at 0.85 V. Inset: Example traces of highly rectifying forward bias (blue) and reverse bias (orange) junctions with rectification ratio of 3.5 and 3.3, respectively.

ductance and current−voltage characteristics of this molecule in ambient, room-temperature conditions with a scanning tunneling microscope (STM) in break-junction mode[23−25] (see SI for details). Briefly, a gold STM tip is brought into contact with a gold-on-mica substrate until a junction conductance of $>5G_0$ ($G_0 = 2e^2/h = 77.6\ \mu S$) is measured. The tip is then withdrawn at a rate of 15 nm/s for 125 ms and held at this displacement for 150 ms before being withdrawn for an additional 75 ms. During the "hold" section, the applied voltage is ramped between ±1 V, while current and voltage are measured simultaneously (Figure 1b). Due to the instability of molecular junctions at high bias at room temperature, many traces cannot sustain a stable molecular plateau during the entire ramp, making higher bias regimes impossible. The $I-V$ procedure is repeated tens of thousands of times, with ∼4% of junctions (5250 out of 131,000 traces) showing a molecular conductance signature during the $I-V$ measurement. A "molecular conductance signature" is defined as a junction that sustains an unbroken conductance plateau throughout the $I-V$ ramp and exhibits the characteristic zero-bias conductance of the molecule in the low-bias regions of the $I-V$ ramp (see SI for details). These selected $I-V$ traces are added together to create a two-dimensional histogram of absolute current against applied voltage (Figure 1c).

Since junctions are equally likely to form with molecules bound in "forward" or "reverse" orientations relative to the applied bias, any rectification is washed out in Figure 1c. We recover the inherent asymmetry of the junction by sorting our data into two sets, based on the magnitude of current in a range of positive biases (+0.75 to +0.80 V) and corresponding negative voltages (−0.75 to −0.80 V). Traces that show larger (smaller) current at positive voltages than negative correspond to molecular junctions in the forward (reverse) orientation. 2D histograms from these sorted data sets are shown in Figure 1d (blue, forward bias) and 1e (orange, reverse bias). To make a quantitative comparison of the histograms, we fit each vertical slice of the histograms to a log-normal distribution and extract the maximum value of the best-fit. These values are plotted as the black and blue $I-V$ curves in Figure 1d (1e) respectively and are also shown overlaid in Figure 1f. The resulting curves represent the statistically most probable $I-V$ curves for this molecule. The forward bias average $I-V$ (blue curve, Figure 1f) overlays the reverse bias $I-V$ (black curve), which has been mirrored in the voltage axis. Both curves show a very linear reverse bias section and a nonlinear forward bias section; the near-identical shape of these curves indicates that sorting recovers the inherent structure in the $I-V$ curves without introducing significant bias. A similar sorting algorithm applied to fully symmetric molecules further confirms this conclusion:

dx.doi.org/10.1021/nl403698m | *Nano Lett.* XXXX, XXX, XXX−XXX

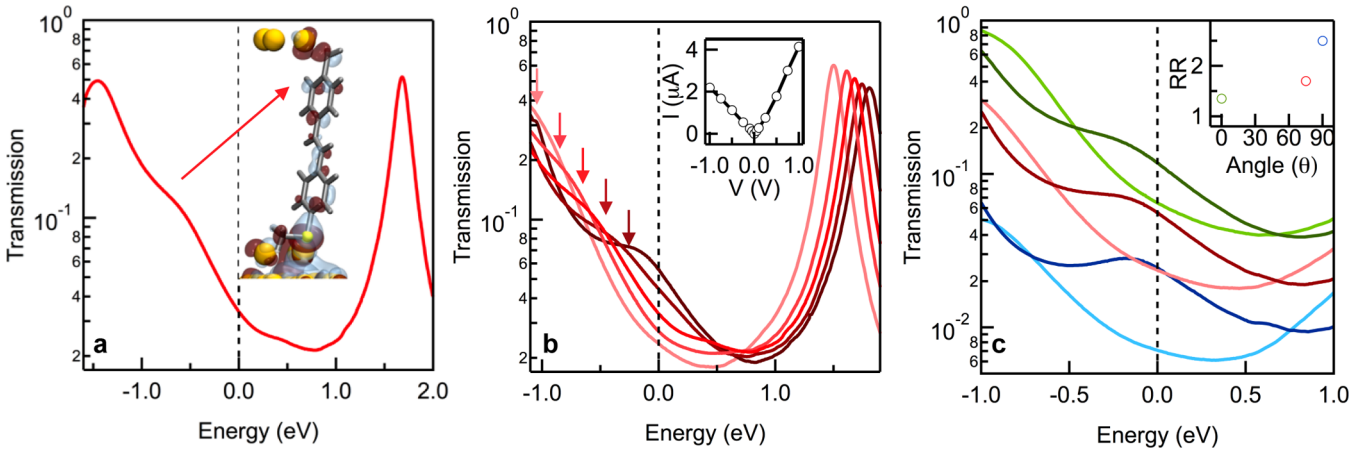

Figure 2. (a) DFT calculated transmission function at zero bias, $T(E,V = 0)$ for molecule **1**. The arrow indicates the position of eigenchannel corresponding to gold−carbon gateway state at −0.5 eV. The dashed line at 0 eV indicates zero-bias Fermi energy for both electrodes. Inset: isosurface plot of the upward moving scattering for the gateway state, showing a significant contribution on the carbon−gold bond. (b) Transmission for molecule **1** as a function of applied bias of −1 V (light red) to +1 V (dark red) in increments of 0.5 V. Arrows point to the gateway state positions at each bias. The dashed line at 0 eV indicates average of left and right chemical potentials. Inset: $I-V$ curve obtained by integrating $T(E,V)$, showing a rectification ratio of 1.8 at 0.85 V. (c) Transmission at −1 V (dark) and +1 V (light) for analogues of molecule **1** with methylsulfide torsional angle $\theta = 0°$ (green) and $\theta = 90°$ (blue) compared to equilibrium geometry (red) which has $\theta = 73°$. Inset: DFT-calculated rectification ratio as a function of the methylsulfide torsion angle.

the separated 2D histograms for these control molecules are identical and do not show rectification (see SI).

Molecule **1** shows an average rectification ratio of 1.7 at an applied bias of 0.85 V (Figure 1f), with rectification evident from ±0.5 V and increasing linearly with increasing bias. Other reported results from single-molecule diodes[2,4] have comparable rectification ratios, but at much higher operational voltages. We find that the maximum observed rectification in selected traces can be much higher than the statistically averaged value, as is shown in sample traces in the inset of Figure 1f. More evidence for junction-to-junction variation of conductance characteristics can be seen in the broad distribution of $I-V$ histograms, especially at high biases (Figure 1d and e). Such variability underscores the need for a statistical measure of rectification over thousands of measurements, to make a meaningful characterization of the high-bias properties of molecular junctions. Our results show that the binding orientation of a molecule in the junction can be ascertained on a trace-by-trace basis, and a statistical measure of rectification in molecules can be established despite the width of the current distributions. Molecule **1** also shows a zero-bias conductance of 5.4×10^{-3} G_0, which is significantly higher than previously reported systems;[4] this suggests that this molecular design could be used as a basis for larger, more complex molecules (or multi-molecule circuits) that enhance functionality while maintaining an experimentally measurable current.

Next, we use ab initio calculations to identify the mechanism behind the diode-like properties of molecule **1** when in a gold junction. We perform density functional theory (DFT) based calculations with a gradient-corrected exchange correlation functional[26] and a nonequilibrium Greens' function approach[27] to optimize the molecular geometry, the details of which have been discussed previously.[22,28] The DFT optimized geometry for molecule **1** bound to gold electrodes with trimer tips (shown in SI) agrees well with published geometries for symmetric gold−carbon and methylsulfide linked molecular backbones.[22,29] Bias-dependent steady-state density matrices are then calculated self-consistently using DFT by integration of the left- and right-moving scattering-states up to their respective chemical potentials, following a standard first-principles approach.[30] At zero applied bias, the left and right chemical potentials are fixed in the three outermost layers of each electrode to their bulk values. As a bias voltage V is applied to the junction, these fixed values are shifted corresponding to the opening of a symmetric bias window (±eV/2). The potential and density are computed under these constraints and are allowed to relax in a central region including the molecule and four layers of gold on each side. The resulting potential profile across the junction is plotted in the SI. $I-V$ characteristics are calculated using the Landauer formula by integrating the bias-dependent transmission functions $T(E,V)$. The zero-bias transmission function for this junction, $T(E,V = 0)$ shown in Figure 2a shows a broad feature at 0.5 eV below the Fermi energy (E_F, dashed line) on the tail of the highest occupied molecular orbital (HOMO) which peaks at −1.4 eV from E_F. The lowest unoccupied molecular orbital (LUMO) is far from E_F (1.8 eV) and is not important to conduction within the experimentally accessible bias window. Although resonance energies are expected to be an underestimated relative to the experiment,[31] we find that DFT is a sufficient level of theory for understanding rectification in these systems.

An isosurface plot of the eigenchannel wave function at −0.5 eV (inset of Figure 2a) shows a "gateway" state derived from the molecular orbital on the gold−carbon bond that is strongly hybridized with molecular π backbone and gold electrode.[22,32] A comparison of transmission functions under an applied bias of −1 V to +1 V in steps of 0.5 V is shown in Figure 2b. We see that the gateway state moves with the chemical potential of the electrode toward E_F under positive bias (dark red curve) and away from E_F for negative bias (light red curve). At every applied bias, the gateway state is largely "pinned" to E_F and moves by 75% of the shift in chemical potential of its adjacent electrode. This shift is not observed for intrinsic molecular resonances, such as the LUMO, which only shifts by 20% of the electrode potential. The high degree of tunability of the pinned gateway state with bias compared to intrinsic molecular orbitals suggests that efficient rectification at low-bias is achieved by bringing a density of states into or out of the bias window. The

dx.doi.org/10.1021/nl403698m | Nano Lett. XXXX, XXX, XXX−XXX

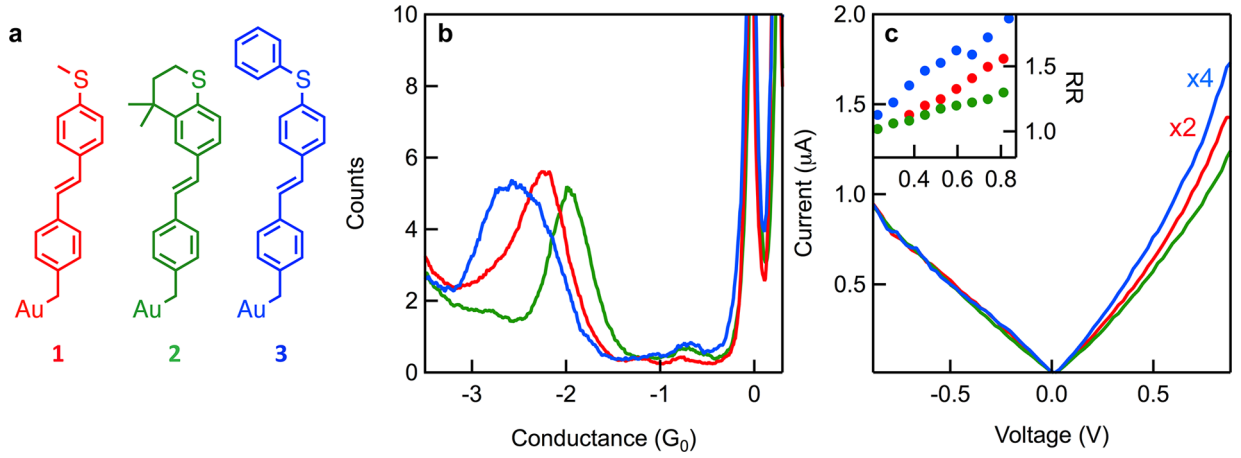

Figure 3. (a) Chemical structures for the original molecular rectifier design (molecule **1**), along with two modified designs, **2** and **3**. All three structures have the same backbone and gateway and differ only in the geometry of the sulfide linker. (b) Log-binned conductance histograms for the three molecules. The decreasing conductance, **2** > **1** > **3**, reflects the decreasing coupling between backbone and sulfur–gold bonds formed by the three sulfide linkers. (c) Scaled, statistically most probable I–V curves for the three molecules. The curves are calculated from log-binned 2D histograms with bin sizes and histogram ranges kept constant. All curves have been scaled to zero-bias conductance of molecule **2**, with the red curve (molecule **1**) multiplied by 2 and the blue curve (molecule **3**) by 4. Inset: Rectification ratio as a function of bias.

large shift seen for the gateway state is a result of strong gold–carbon hybridization, which leads to a high polarizability and relatively flat potential profile near the gold–carbon bond under bias (see SI). The calculated I–V curve for this junction (inset, Figure 2b) is asymmetric with a rectification ratio of 1.8 at 0.85 V, very close to the experimental value of 1.7. While the magnitude of computed current is somewhat overestimated (as expected from DFT-based transport calculations),[28] the much smaller error in the position of the gateway state due to its relatively strong coupling to the electrodes[32] leads to striking agreement between the experimental and the theoretical rectification ratio. Our calculations indicate that rectification in molecule **1** is a consequence of the gateway modulation and suggests that higher rectification ratios can be achieved by tuning the response of this state to bias.

To explore the tunability of this molecular diode design, we develop a tight-binding model to identify parameters that govern rectification ratio (see SI). A similar theoretical approach has previously been used to explain negative differential resistances in atomic wire junctions using carbon-nanotube electrodes.[33] Our model suggests that the coupling between the two sides of the molecule plays an important role in the shape and high-bias shift of the gateway state. In particular, our model predicts that the rectification ratio should increase as the coupling between the backbone π-system and the methylsulfide linker decreases (see SI). We explore the possibility of tuning the coupling by varying the carbon–sulfur–gold torsional angle θ between the backbone π-system and the methylsulfide linker of molecule **1**.[34] We perform DFT calculations on two analogues of molecule **1**, with the methylsulfide linker constrained parallel (θ = 0°) or perpendicular (θ = 90°) to the plane of the stilbene backbone. Figure 2c compares the resulting high bias transmission functions, $T(E,V = +1\ \mathrm{V})$ and $T(E,V = -1\ \mathrm{V})$ for the three structures. All three clearly show the presence of a gateway state close to E_F, which moves under an applied bias. The structure with θ = 0°, which yields the highest gateway-backbone coupling, has the lowest rectification (1.3); in contrast, the structure with θ = 90°, which has the lowest intramolecular coupling, exhibits a significant rectification ratio of 2.6.

Having established the mechanism for rectification and a route for its optimization, we now design molecules to experimentally test these predictions. The methylsulfide linker in our original rectifier provides a convenient method of achieving this goal. The coupling of the π-system through the gold–sulfur donor–acceptor bond varies with their relative orientation,[34] and control of this relative orientation should therefore result in tunable rectification. In Figure 3a, we show two molecules with better (**2**) or worse (**3**) π–gold–sulfur coupling than **1** based on their chemical structures. The methylsulfide group in **2** is locked in-plane with the molecular backbone through the saturated six-membered ring. This ring orients the methylsulfide group nearly parallel to the backbone's π-system and gives near-maximal coupling of the gold–sulfur bond to the backbone, analogous to the θ = 0° structure discussed earlier. Molecule **3** has a phenylsulfide replacing the methylsulfide group, which decreases the electronic coupling across the sulfide linker when compared with **1**.[34]

Our measurements of the zero-bias conductance ($V_{applied}$ < 100 mV) show that molecules **2** and **3** conduct higher and lower than molecule **1** (Figure 3b) and confirm that we are able to tune coupling between the backbone and the gold–sulfur bond through chemical modifications. The scaled I–V curves for this family of molecules (Figure 3c) show a linear reverse bias regime for all three molecules, which results from a relatively flat transmission function within the integration window, consistent with the observation that the gateway is moving away from E_F. On the forward bias side, the curves are all nonlinear, with **3** (blue) showing the most curvature due to the influence of a more prominent gateway state. For each of these curves, we determine a rectification ratio as a function of applied bias by dividing forward bias current with the corresponding reverse bias current (inset, Figure 3c). For all three molecules, rectification increases linearly with applied bias, with significant asymmetry seen as low as ±0.5 V. The molecule with the poorest coupling, **3**, rectifies the most, while **2**, with the strongest coupling, rectifies the least. More importantly, we have demonstrated that, by increasing the methylsulfide torsion angle, we can increase the asymmetry in the measured I–V curves by over a factor of 3. This is

dx.doi.org/10.1021/nl403698m | *Nano Lett.* XXXX, XXX, XXX–XXX

experimental verification of a rationally designed family of rectifiers whose asymmetry can be tuned by varying a single parameter through chemical design.

The results presented in this paper introduce a new mechanism for rectification based on the electrostatic modulation of a gold−carbon gateway state. The relative simplicity of this mechanism is highlighted by the fact that rectification can be tuned through molecular design. The tunability of this design combined with the low operational voltages and high zero-bias conductances achieved can facilitate future designs that optimize performance with larger, more complicated chemical structures. More broadly, our results establish localized gateway states as a design element whose unique high-bias properties can be integrated into existing molecular structures to create new functionality.

■ ASSOCIATED CONTENT

Supporting Information

Additional information, methods, and figures. This material is available free of charge via the Internet at http://pubs.acs.org.

■ AUTHOR INFORMATION

Corresponding Authors

*E-mail: neaton@lbl.gov.
*E-mail: cn37@columbia.edu.
*E-mail: lv2117@columbia.edu.

Present Address

J.S.M.: Department of Chemistry, Duke University, Durham, North Carolina 27708, United States.

Author Contributions

A.B., P.D., and Q.C. contributed equally.

Notes

The authors declare no competing financial interest.

■ ACKNOWLEDGMENTS

We thank Dr. Mark S. Hybertsen for fruitful discussions. This work has been supported in part by the NSF Career Award (CHE-07-44185), Packard Foundation. A.B. acknowledges support from the National Science Foundation Graduate Research Fellowship under grant no. DGE-07-07425. Portions of this work were performed at the Molecular Foundry and supported by the Division of Materials Sciences and Engineering (Theory FWP), both under the auspices of the Office of Basic Energy Sciences of the U.S. Department of Energy under contract no. DE-AC02-05CH11231. We thank the National Energy Research Scientific Computing center for computational resources. This work was also supported as part of the Center for Re-Defining Photovoltaic Efficiency Through Molecular-Scale Control, an Energy Frontier Research Center funded by the U.S. Department of Energy (DOE), Office of Science, Office of Basic Energy Sciences under award number DE-SC0001085.

■ REFERENCES

(1) Aviram, A.; Ratner, M. A. *Chem. Phys. Lett.* **1974**, *29*, 277−283.
(2) Elbing, M.; Ochs, R.; Koentopp, M.; Fischer, M.; von Hanisch, C.; Weigend, F.; Evers, F.; Weber, H. B.; Mayor, M. *Proc. Natl. Acad. Sci. U.S.A.* **2005**, *102*, 8815−8820.
(3) Taylor, J.; Brandbyge, M.; Stokbro, K. *Phys. Rev. B* **2003**, *68*, 1211011−1211014.
(4) Díez-Pérez, I.; Hihath, J.; Lee, Y.; Yu, L.; Adamska, L.; Kozhushner, M. A.; Oleynik, I. I.; Tao, N. *Nat. Chem.* **2009**, *1*, 635−641.
(5) Stadler, R.; Geskin, V.; Cornil, J. *J. Phys.: Condens. Matter* **2008**, *20*, 37.
(6) Ellenbogen, J. C.; Christopher Love, J. *Proc. IEEE* **2000**, *88*, 386−426.
(7) Tao, N. *Nat. Nanotechnol.* **2006**, *1*, 173−181.
(8) McCreery, R. L.; Bergren, A. J. *Adv. Mater.* **2009**, *21*, 4303−4322.
(9) Hybertsen, M. S.; Venkataraman, L.; Klare, J. E.; Whalley, A. C.; Steigerwald, M. L.; Nuckolls, C. *J. Phys.: Condens. Matter* **2008**, *20*, 374115.
(10) Mujica, V.; Ratner, M. A.; Nitzan, A. *Chem. Phys.* **2002**, *281*, 147−150.
(11) Stadler, R.; Geskin, V.; Cornil, J. *J. Phys.: Condens. Matter* **2008**, *20*, 374105.
(12) Yee, S. K.; Sun, J. B.; Darancet, P.; Tilley, T. D.; Majumdar, A.; Neaton, J. B.; Segalman, R. A. *ACS Nano* **2011**, *5*, 9256−9263.
(13) Lortscher, E.; Gotsmann, B.; Lee, Y.; Yu, L. P.; Rettner, C.; Riel, H. *ACS Nano* **2012**, *6*, 4931−4939.
(14) Dhirani, A.; Lin, P.-H.; Guyot-Sionnest, P.; Zehner, R.; Sita, L. *J. Chem. Phys.* **1997**, *106*, 5249.
(15) Reed, M. A.; Zhou, C.; Muller, C. J.; Burgin, T. P.; Tour, J. M. *Science* **1997**, *278*, 252−254.
(16) Metzger, R. M. *Chem. Rev.* **2003**, *103*, 3803−3834.
(17) Kushmerick, J.; Holt, D.; Yang, J.; Naciri, J.; Moore, M.; Shashidhar, R. *Phys. Rev. Lett.* **2002**, *89*, 086802.
(18) Guédon, C. M.; Valkenier, H.; Markussen, T.; Thygesen, K. S.; Hummelen, J. C.; van der Molen, S. J. *Nat. Nanotechnol.* **2012**, *7*, 305−9.
(19) Tian, W.; Datta, S.; Hong, S.; Reifenberger, R.; Henderson, J. I.; Kubiak, C. P. *J. Chem. Phys.* **1998**, *109*, 2874.
(20) Taylor, J.; Brandbyge, M.; Stokbro, K. *Phys. Rev. Lett.* **2002**, *89*, 1383011−1383014.
(21) Park, Y. S.; Whalley, A. C.; Kamenetska, M.; Steigerwald, M. L.; Hybertsen, M. S.; Nuckolls, C.; Venkataraman, L. *J. Am. Chem. Soc.* **2007**, *129*, 15768−15769.
(22) Chen, W.; Widawsky, J. R.; Vázquez, H.; Schneebeli, S. T.; Hybertsen, M. S.; Breslow, R.; Venkataraman, L. *J. Am. Chem. Soc.* **2011**, *133*, 17160−17163.
(23) Xu, B. Q.; Tao, N. J. *Science* **2003**, *301*, 1221−1223.
(24) Venkataraman, L.; Klare, J. E.; Tam, I. W.; Nuckolls, C.; Hybertsen, M. S.; Steigerwald, M. L. *Nano Lett.* **2006**, *6*, 458−462.
(25) Widawsky, J. R.; Kamenetska, M.; Klare, J.; Nuckolls, C.; Steigerwald, M. L.; Hybertsen, M. S.; Venkataraman, L. *Nanotechnology* **2009**, *20*, 434009.
(26) Perdew, J. P.; Burke, K.; Wang, Y. *Phys. Rev. B* **1996**, *54*, 16533.
(27) Brandbyge, M.; Mozos, J. L.; Ordejon, P.; Taylor, J.; Stokbro, K. *Phys. Rev. B* **2002**, *65*, 165401.
(28) Darancet, P.; Widawsky, J. R.; Choi, H. J.; Venkataraman, L.; Neaton, J. B. *Nano Lett.* **2012**, *12*, 6250−6254.
(29) Frei, M.; Aradhya, S. V.; Hybertsen, M. S.; Venkataraman, L. *J. Am. Chem. Soc.* **2012**, *134*, 4003−4006.
(30) Choi, H. J.; Marvin, L. C.; Steven, G. L. *Phys. Rev. B* **2007**, *76*, 155420.
(31) Cohen, A. J.; Mori-Sánchez, P.; Yang, W. *Science* **2008**, *321*, 792−794.
(32) Widawsky, J. R.; Chen, W.; Vazquez, H.; Kim, T.; Breslow, R.; Hybertsen, M. S.; Venkataraman, L. *Nano Lett.* **2013**, *13*, 2889−2894.
(33) Khoo, K. H.; Neaton, J.; Son, Y. W.; Cohen, M. L.; Louie, S. G. *Nano Lett.* **2008**, *8*, 2900−2905.
(34) Park, Y. S.; Widawsky, J. R.; Kamenetska, M.; Steigerwald, M. L.; Hybertsen, M. S.; Nuckolls, C.; Venkataraman, L. *J. Am. Chem. Soc.* **2009**, *131*, 10820−10821.